This paper is available on line at http://www.mcponline.org

Quantitative Phosphoproteomics Analysis Reveals a Key Role of Insulin Growth Factor 1 Receptor (IGF1R) Tyrosine Kinase in Human Sperm Capacitation*[S]

Jing Wang‡, Lin Qi‡, Shaoping Huang‡, Tao Zhou‡, Yueshuai Guo‡, Gaigai Wang‡, Xuejiang Guo‡§, Zuomin Zhou‡§, and Jiahao Sha‡

One of the most important changes during sperm capacitation is the enhancement of tyrosine phosphorylation. However, the mechanisms of protein tyrosine phosphorylation during sperm capacitation are not well studied. We used label-free quantitative phosphoproteomics to investigate the overall phosphorylation events during sperm capacitation in humans and identified 231 sites with increased phosphorylation levels. Motif analysis using the NetworKIN algorithm revealed that the activity of tyrosine phosphorylation kinases insulin growth factor 1 receptor (IGF1R)/insulin receptor is significantly enriched among the up-regulated phosphorylation substrates during capacitation. Western blotting further confirmed inhibition of IGF1R with inhibitors GSK1904529A and NVP-AEW541, which inhibited the increase in tyrosine phosphorylation levels during sperm capacitation. Additionally, sperm hyperactivated motility was also inhibited by GSK1904529A and NVP-AEW541 but could be up-regulated by insulin growth factor 1, the ligand of IGF1R. Thus, the IGF1R-mediated tyrosine phosphorylation pathway may play important roles in the regulation of sperm capacitation in humans and could be a target for improvement in sperm functions in infertile men. ***Molecular & Cellular Proteomics 14: 10.1074/mcp.M114.045468, 1104–1112, 2015.***

Austin (1) and Chang (2) discovered that sperm must reside in the female genital tract for a specific period of time to acquire the ability to fertilize an egg and named this process "capacitation." During capacitation, several biochemical changes occur, including enhancement of tyrosine phosphorylation (3), increased intracellular Ca^{2+} and cAMP levels (4), hyperactivated motility (5), and increased membrane plasma permeability (6). Mature sperm are highly differentiated and specialized cells, there is almost no transcription, and the genomic ribosome is inactive (5). Therefore, regulation of proteins at the level of post-translational modification is expected to play important roles in sperm functions. In mammalian sperm, phosphorylated proteins, protein kinases, and phosphatases are reported to function in sperm motility, capacitation, and acrosome reaction (7, 8). Tyrosine phosphorylation and dephosphorylation are required for sperm to reach, bind, penetrate, and fuse with the oocyte (5). Tyrosine-phosphorylated proteins have been found in human (9), monkey (10), rat (11), and mouse (12) sperm. The sperm tail is the main location of protein tyrosine phosphorylation, and tyrosine phosphorylation of the sperm tail is related to hyperactivated motility (13). However, the mechanism of protein tyrosine phosphorylation regulation in sperm capacitation is not well studied.

With high throughput ability, proteomics has been used to characterize phosphorylation in sperm. For the human sperm, Ficarro *et al.* (14) used two-dimensional polyacrylamide gel electrophoresis (PAGE), anti-phosphotyrosine antibody labeling, and tandem mass spectrometry (MS/MS) to identify tyrosine phosphoproteins during capacitation. They identified a total of five tyrosine phosphorylation sites, 56 serine phosphorylation sites, and two threonine phosphorylation sites. Because of the low abundance of phosphorylation, recent studies used an enrichment approach to identify phosphorylation sites. In rodents, Platt *et al.* (15) labeled uncapacitated and capacitated mouse sperm protein using an isotope labeling reagent based on Fisher esterification and quantified 55 phosphorylation sites during sperm capacitation. Baker *et al.* (16), using a rat model, quantified 288 phosphorylated peptides during sperm capacitation. However, the regulation of phosphorylation in human sperm is not well understood, and rodents may not be good models for humans. It is thus important to study and elucidate the regulation of phosphorylation during capacitation in human sperm.

From the ‡State Key Laboratory of Reproductive Medicine, Collaborative Innovation Center of Genetics and Development, Department of Histology and Embryology, Nanjing Medical University, Nanjing 210029, China

Received, October 6, 2014, and in revised form, February 14, 2015
Published, MCP Papers in Press, February 19, 2015, DOI 10.1074/mcp.M114.045468

Author contributions: X.G., Z.Z., and J.S. designed research; J.W., L.Q., S.H., Y.G., and G.W. performed research; T.Z., X.G., and Z.Z. analyzed data; J.W., T.Z., X.G., Z.Z., and J.S. wrote the paper.

To quantify phosphorylation changes and identify functional kinases during human sperm capacitation, we used label-free quantitative phosphoproteomics to investigate the overall phosphorylation events. A total of 3,303 phosphorylated sites, corresponding to 986 phosphorylated proteins, were identified using immobilized metal affinity chromatography (IMAC)-TiO_2 phosphopeptide continuous enrichment methods by liquid chromatography (LC)-MS/MS; the phosphorylation levels of 231 sites were increased significantly. Motif analysis and an inhibition assay showed essential functions of insulin growth factor 1 receptor (IGF1R)[1] as a tyrosine receptor kinase in tyrosine phosphorylation and hyperactivated motility during sperm capacitation.

EXPERIMENTAL PROCEDURES

Sperm Collection—Prior to sample collection, this study was approved by the Ethics Committee of Nanjing Medical University. The sperm subjected to proteomics analysis were obtained from 32 healthy male volunteers with a mean age of 30 ± 4 years old (mean ± S.D.). These men had proven fertility and normal semen quality as assessed based on World Health Organization criteria.

The semen samples were obtained by masturbation after at least 3 days of abstinence. The samples were ejaculated into sterile containers and allowed to liquefy for at least 30 min before being processed by centrifugation (2,000 × *g* for 5 min) in a 60% Percoll gradient (GE Healthcare, Waukesha, WI) to remove seminal plasma, immature germ cells, and non-sperm cells (mainly epithelial cells) as described by Gandini *et al.* (17). The human sperm were gently isolated into Biggers-Whitten-Whittingham medium, and then the purified sperm were thrice washed in phosphate-buffered saline (PBS), pH7.2 at 2,000 × *g* for 5 min before subsequent proteomics analysis. The sperm samples were divided into two parts; one part was directly collected as a non-capacitation sample, and the other part was cultured in capacitation medium consisting of human tubal fluid (In-VitroCare, Frederick, MD) supplemented with 1% bovine serum albumin (BSA; Sunshine, Nanjing, China) for 2 h. The combined human tubal fluid-BSA medium is widely used for *in vitro* sperm capacitation because it can improve the pregnancy rate of *in vitro* fertilization (18).

Phosphopeptide Enrichment—The sperm were lysed in urea lysis buffer (8 M urea,75 mM sodium chloride, 50 mM Tris, 1% v/v cocktail (Halt Protease Inhibitor Cocktail; Pierce, Rockford, IL), 1 mM natrium fluoride, 1 mM β-glycerophosphate, 1 mM sodium orthovanadate, 10 mM sodium pyrophosphate, pH 8.2). Triplicate lysates were centrifuged at 40,000 × *g* for 60 min (4 °C) following sonication for 10 s. Each pooled 1-mg protein sample from capacitated or uncapacitated sperm was used for subsequent phosphorylation studies. To reduce disulfide bonds, the proteins were incubated with dithiothreitol at a 5 mM final concentration for 25 min at 56 °C. After the protein mixtures cooled to room temperature, iodoacetamide was added to a 14 mM final concentration. The protein mixture was diluted (1:5) in 25 mM Tris-HCl, pH 8.2 to reduce the concentration of urea to 1.6 M. The proteins were then digested by trypsin at 37 °C overnight and subsequently quenched by addition of trifluoroacetic acid (TFA). The peptides were desalted using a Sep-Pak column from Waters Co. (Milford, MA).

IMAC beads were thrice washed with 1 ml of IMAC binding buffer (40% acetonitrile (ACN) (v/v) and 25 mM formic acid in H_2O) and prepared as a 50% slurry in the same buffer. The desalted peptides were dissolved in 120 μl of IMAC binding buffer and then transferred to the prepared 10 μl of IMAC beads. The desalted peptides were incubated with IMAC beads for 60 min at room temperature, and then the supernatants were dried by vacuum centrifugation and used for subsequent TiO_2 enrichment. The IMAC beads were washed with 120 μl of IMAC binding buffer. The phosphopeptides were eluted by incubation for 15 min with 40 μl of IMAC elution buffer (50 mM K_2HPO_4/NH_4OH, pH 10.0), neutralized with 10% formic acid, and then purified on C_{18} StageTips for subsequent identification (19).

For subsequent TiO_2 enrichment, the peptide samples after IMAC enrichment were resolved in 200 μl of loading buffer (65% ACN and 2% TFA saturated by glutamic acid) and incubated with TiO_2 beads (GL Sciences, Tokyo, Japan) at a ratio of 1:4 (peptides:beads). The incubated beads were then washed with 800 μl of wash buffer I (65% ACN and 0.5% TFA) and wash buffer II (65% ACN and 0.1% TFA). The bound peptides were eluted once with the 200 μl of elution buffer I (300 mM NH_4OH and 50% ACN) and twice with 200 μl of elution buffer II (500 mM NH_4OH and 60% ACN). The eluates were dried down and then desalted on C_{18} StageTips (19).

Liquid Chromatography-Tandem Mass Spectrometry—The IMAC and TiO_2 enriched phosphopeptides were analyzed using an LTQ Orbitrap Velos (ThermoFinnigan, San Jose, CA) coupled directly to an LC column. The trap column effluent was transferred to a reverse-phase microcapillary column (0.075 × 150 mm, Acclaim® PepMap100 C_{18} column, 3 μm, 100 Å; Dionex, Sunnyvale, CA). Reverse-phase separation of peptides was performed using buffer A (2% ACN and 0.5% acetic acid) and buffer B (80% ACN and 0.5% acetic acid) under a 238-min gradient (4–30% buffer B for 208 min, 30–45% buffer B for 20 min, 45–100% buffer B for 1 min, 100% buffer B for 8 min, and 100–4% buffer B for 1 min). An MS survey scan was obtained for the mass-to-charge ratio (*m/z*) range 350–1,800, and MS/MS spectra were acquired in the LTQ for the 20 most intense ions from the survey scan (determined using Xcalibur mass spectrometer software in real time). Dynamic mass exclusion windows of 60 s were used with siloxane (m/z = 445.120025) as a lock mass. Uncapacitated and capacitated sperm samples were analyzed alternately to avoid systematic variation. The experiments were repeated three times.

Database Searching and Data Interpretation—Raw files were processed using MaxQuant (version 1.3.0.5) (20) and searched against the UniProt human protein database (version 2012_5; 55,269 sequences) (21). Enzyme specificity was considered to be full cleavage by trypsin, and two maximum missed cleavage sites were permitted. The minimum peptide length required was six amino acids. Carbamidomethylation (Cys) was set as a fixed modification. Variable modifications included oxidation (Met), acetylation (protein N terminus), and phosphorylation (Ser/Thr/Tyr). Mass tolerances for precursor ions and fragment ions were set to 20 ppm and 0.5 Da, respectively. The false discovery rate (FDR) of the identification was estimated by searching against the databases with the reversed sequences. The site, peptide, and protein FDRs were all set to 0.01. The minimum score required for the phosphorylation site was 30 to obtain reliable results. Protein phosphorylation was quantified using the peptide-extracted ion chromatograms embedded in MaxQuant (22). Student's *t* test was used for statistical comparisons. The expression changes of phosphorylation sites with a p value less than 0.05 and a -fold change greater than 1.5 were considered statistically significant.

Bioinformatics Analysis—Gene ontology annotations can provide a functional overview for a specific protein list (23). Thus, we performed gene ontology enrichment analysis for the proteins with up-regulated phosphorylation sites using ToppGene (24). The human genome was set as background, and an adjusted p value (using the Bonferroni

[1] The abbreviations used are: IGF1R, insulin growth factor 1 receptor; CASA, computer-aided sperm analysis; FDR, false discovery rate; IGF1, insulin growth factor 1; INSR, insulin receptor; AKAP, protein kinase A-anchoring protein; CABYR, calcium-binding tyrosine phosphorylation-regulated.

method) less than 0.05 was used for significant enrichment. The protein-protein interaction network for the proteins with up-regulated phosphorylation sites was annotated using the STRING database (version 9.1) (25).

Prediction of Regulatory Kinases—To investigate the regulatory interactions between kinases and phosphorylated sites, we used NetworKIN (version 2.0) (26) to annotate the relationships between predicted kinases and phosphorylated sites. All identified phosphorylated sites were submitted to NetworKIN for prediction of *in vivo* kinase-substrate relationships. The NetworKIN algorithm combines kinase consensus motifs and considers protein-protein interactions. The cutoff for the NetworKIN score was set to 3. To further determine kinases with enrichment of significantly up-regulated phosphorylation sites, we performed enrichment analysis for each predicted kinase using Fisher's exact test. All identified phosphorylation sites were set as background. The cutoff for significant kinases was an FDR value less than 0.05.

Kinase Inhibition Assays—An IGF1R/INSR kinase inhibitor (GSK1904529A; Selleck Chemicals LLC, Houston, TX) and an IGF1R kinase inhibitor (NVP-AEW541; Selleck Chemicals LLC) were used for kinase function studies. Sperm samples were incubated in capacitating medium containing 1% (v/v) dimethyl sulfoxide (DMSO) with GSK1904529A at 30 μM, NVP-AEW541 at 5 μM, IGF1 (Sigma, St. Louis, MO) at 50 or 100 ng/ml, or insulin (Sigma) at 10 or 100 μg/ml. Capacitating medium containing 1% (v/v) DMSO only was used as a control. After incubation for 0 or 6 h at 37 °C in a 5% CO_2 incubator, the sperm hyperactivated motility was detected using computer-aided sperm analysis (CASA; IVOS, Hamilton Thorne Biosciences, Beverly, MA). Aliquots of semen samples (10 μl) were placed into a Makler counting chamber (Sefi Medical Instruments Ltd., Haifa, Israel), and at least 300 sperm cells were evaluated at each incubation time by phase-contrast microscopy. Hyperactivated motility analysis was performed using the CASA system (Sperm Class Analyzer, Barcelona, Spain).

Immunoblotting—The samples (15 μg of total protein) were subjected to electrophoresis for ~2 h at a constant voltage of 100 V using 10–20% gradient gels (Bio-Rad, Hercules, CA). After electrophoresis, gels were electroblotted onto a polyvinylidene fluoride (PVDF) membrane (Bio-Rad) for 2 h at a constant current of 300 mA using a Mini Trans-Blot system (Bio-Rad). Following transfer, PVDF membrane were blocked with 5% milk (Bio-Rad) in Tris-buffered saline (TBS), pH 7.4 for 2 h before incubation with mouse anti-phosphotyrosine antibody (1:1,000; Millipore, Bedford, MA) diluted in primary antibody dilution buffer at 4 °C overnight. Membranes were washed thrice in TBS-Tween 20 and then probed with peroxidase-conjugated goat anti-mouse immunoglobulin G (IgG; 1:1,000; Beijing Zhongshan Biotechnology Co., China) for 1 h at 37 °C. After thrice washing, an enhanced chemoluminescence reaction kit (Amersham Biosciences, Piscataway, NJ) was used in a darkroom for 10 min.

RESULTS

Protein Tyrosine Phosphorylation Changes during Sperm Capacitation—Increased protein tyrosine phosphorylation is a marker for sperm capacitation (27). After incubation in capacitation medium for 1–3 h, we analyzed the levels of tyrosine-phosphorylated proteins via immunoblotting using anti-phosphotyrosine antibody (Fig. 1). Immunoblotting showed a significant increase in tyrosine phosphorylation with a peak level at 2 h. Clear increases in the 90- and 70-kDa bands of tyrosine-phosphorylated proteins were observed. Therefore, we used sperm incubated for 0 (control) and 2 h in capacitation medium for subsequent quantitative phosphoproteomics analysis.

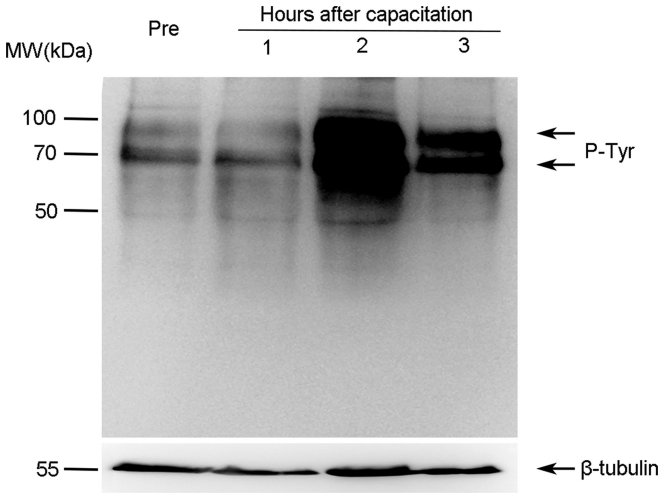

FIG. 1. **Changes of protein tyrosine phosphorylation during human sperm capacitation.** Human sperm were cultured without (Pre) or with capacitation for 1, 2, or 3 h. Protein tyrosine phosphorylation levels were analyzed via immunoblotting using the anti-phosphotyrosine (*P-Tyr*) antibody. β-Tubulin was used as an internal reference.

Label-free Quantitative Phosphoproteomics Profiling—A total of 3,303 phosphorylated sites (FDR < 1%) corresponding to 986 phosphorylated proteins were identified from LC-MS/MS analyses in three technical replicates (supplemental Data 1). To quantify more phosphorylation sites, each experiment used two continuous enrichment methods involving IMAC and TiO_2 phosphopeptide enrichment (Fig. 2*A*). Quantitative analysis of the proteomics data revealed an increase in the phosphorylation levels of 231 sites on 147 proteins and a decrease of 16 sites on 14 proteins (-fold change >1.5, $p < 0.05$) in capacitated sperm compared with uncapacitated sperm (Fig. 2*B*). Twenty-five sites on 18 proteins showed an increase, and one site showed a decrease in tyrosine phosphorylation. Phosphorylation of serine (Ser), threonine (Thr), and tyrosine (Tyr) occupied 77.3, 18.1, and 4.5% of total phosphorylation sites, respectively. Among the up-regulated phosphorylation sites, the percentages of Ser, Thr, and Tyr were 76.6, 12.6, and 10.8%, respectively (Fig. 2*C*).

Functional Annotation—The 147 proteins with up-regulated phosphorylation sites were mapped to 119 unique Entrez gene identities and subjected to the ToppGene database for gene ontology enrichment analysis. For cellular components, the most enriched gene ontology terms were "cilium" (20 genes) and "axoneme" (eight genes; supplement Data 2). Consistent with cellular components, the most enriched biological process was also "cilium movement" (seven genes). The increase in tyrosine phosphorylation in sperm tails after capacitation can be explained by the increased phosphorylation levels of microtubular or flagellar proteins. To further investigate the relationships among these proteins, we constructed a protein-protein interaction network using the STRING database. As shown in Fig. 3, 56 genes are connected with 61 paired relationships. The STRING database

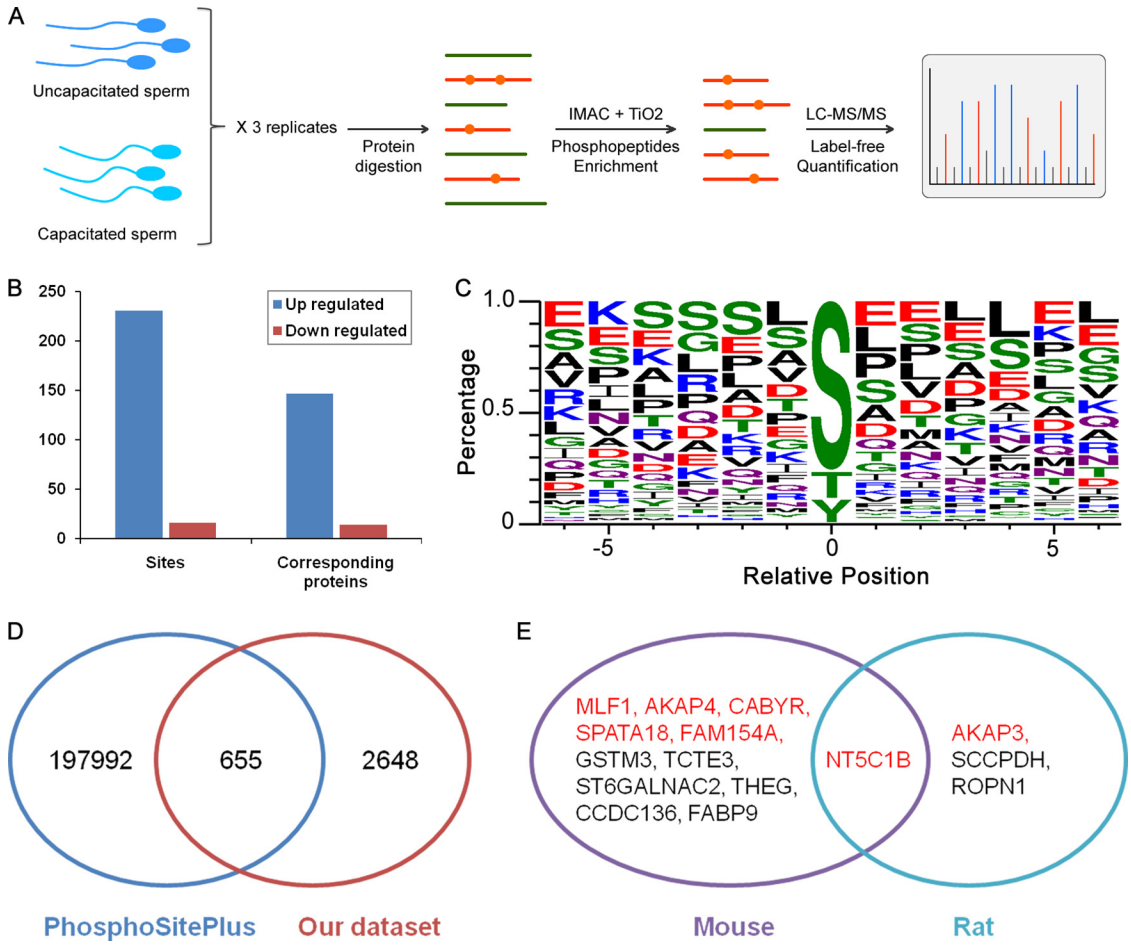

FIG. 2. **Quantitative phosphoproteomics profiling of human sperm capacitation.** *A*, workflow of quantitative phosphoproteomics analysis. *B*, summary of differentially expressed sites and the corresponding proteins. *C*, WebLogo of significantly up-regulated phosphotyrosine sites. *D*, comparison of our identified sites in human sperm with the PhosphoSitePlus database. *E*, comparison of the up-regulated sites of our data set with mouse and rat data sets. Genes with *red* color overlapped with our data set.

provides known and predicted protein interactions, including physical and functional associations (the detailed relationships and corresponding scores are listed in supplement Data 3). Many substrates are directly associated with sperm capacitation and motility. For example, CABYR, a calcium-binding and tyrosine phosphorylation-regulated protein, is a key gene for capacitation and acrosome reaction. CABYR is annotated to interact with AKAP3 and AKAP4. AKAP3 and AKAP4 are both kinase anchor proteins and play roles in motility and head-associated functions such as capacitation and the acrosome reaction.

Prediction of Dominant Kinase—Sequences around phosphorylation sites can be recognized by specific kinases. The NetworKIN database has integrated the sequence bias information around phosphorylation sites with the protein association network information to improve prediction of cellular kinase-substrate relationships (26). Thus, we applied NetworKIN analysis to identify candidate kinases involved in the phosphorylation of capacitated sperm. Based on the 231 up-regulated phosphorylation sites, we found that IGF1R and INSR are the only significantly enriched kinases (FDR $<$ 0.05). IGF1R and INSR are both tyrosine phosphorylation kinases and share the same substrates. IGF1R and INSR are predicted to regulate the same 13 substrate sites, which could not be distinguished (Table I). These substrate sites are located among 10 proteins, including gene products of ACSL1, AKAP3, AKAP4, ALS2CR11, CABYR, EML4, MKI67IP, PGK1, RSHL2, and TOMM34 (Table I).

Kinase Inhibition and Stimulation Assay of Hyperactivated Motility—During capacitation, sperm obtain an increased level of tyrosine phosphorylation and hyperactivated motility. A previous study showed that the enhancement of hyperactivated motility is associated with the stimulation of tyrosine phosphorylation in the sperm tail (13). GSK1904529A is a small molecule kinase inhibitor that inhibits both IGF1R and INSR. This compound is a reversible ATP-competitive inhibitor (28). We found that treatment with GSK1904529A significantly inhibits hyperactivated motility during sperm capacitation (6.67 $\pm$ 1.03 *versus* 18.00 $\pm$ 0.89%). However, when human sperm are incubated with IGF1 or insulin, which can

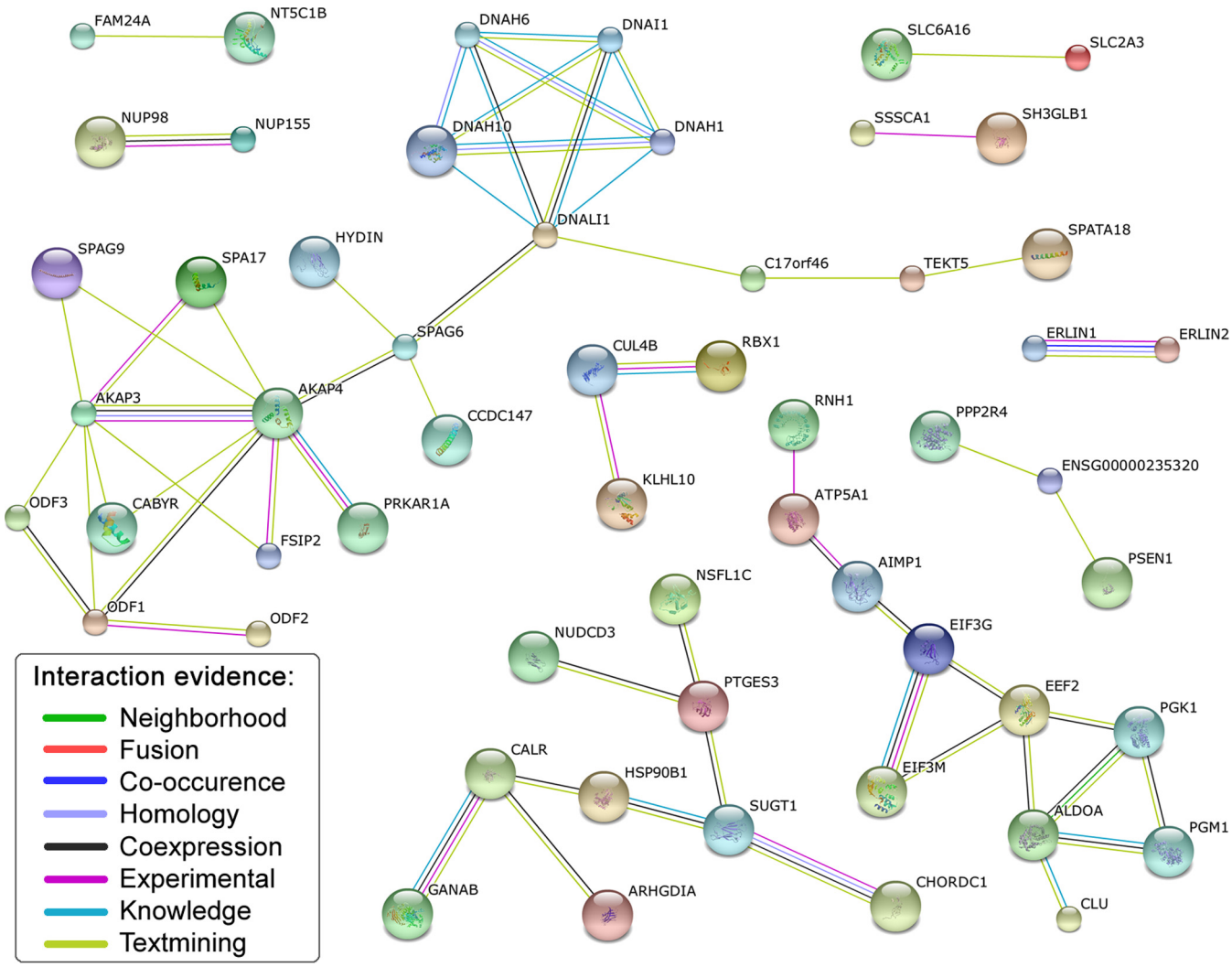

FIG. 3. **Network of proteins with up-regulated sites.** A total of 56 genes are connected with 61 paired relationships annotated by STRING database. The relationships among proteins are derived from evidence that includes coexpression, co-occurrence, experimental, fusion, homology, knowledge, neighborhood, and text mining (as shown in the legend with different color).

specifically stimulate their receptors (IGF1R or INSR), only IGF1 enhanced hyperactivated motility at 6 h (21.67 ± 1.37 *versus* 18.00 ± 0.89% at 100 ng/ml) in a concentration-dependent manner (Fig. 4*A*). Insulin has no effect on hyperactivated motility (Fig. 4*C*). These results suggest that only IGF1R might be essential for sperm hyperactivated motility.

To further study the function of IGF1R in hyperactivated motility during human sperm capacitation, NVP-AEW541, a small molecule kinase inhibitor specific for IGF1R kinase but not INSR kinase, was used (29). CASA showed that NVP-AEW541 (5 μM) significantly inhibited hyperactivated motility after a 6-h incubation (5.00 ± 1.79 *versus* 17.67 ± 0.52%; Fig. 4*B*). When sperm were incubated with both IGF1 and NVP-AEW541, hyperactivated motility was increased compared with NVP-AEW541 alone (25.67 ± 2.07 *versus* 5.00 ± 1.79%). These results suggest that IGF1 can induce sperm hyperactivated motility, which can be inhibited by specific inhibition of its receptor (IGF1R).

Role of IGF1R in Tyrosine Phosphorylation during Human Sperm Capacitation—As CASA showed essential roles of IGF1R in hyperactivated sperm motility, it is possible that it may also play important functions in tyrosine phosphorylation regulation. With the effective concentration of GSK1904529A or NVP-AEW541 used in CASA, we found that tyrosine phosphorylation was almost completely inhibited after inhibition of IGF1R with either GSK1904529A (30 μM) or NVP-AEW541 (5 μM) (Fig. 5). Thus, IGF1R also plays an essential role in the regulation of tyrosine phosphorylation during sperm capacitation.

DISCUSSION

Protein phosphorylation regulation during capacitation is crucial for sperm functions, and the increase in tyrosine phosphorylation is well known to be a marker of capacitation (27). To understand the overall regulation of phosphorylation during sperm capacitation, several groups have used proteomics technology to quantify changes, but only a few phosphoryla-

TABLE I
Up-regulated tyrosine-phosphorylated sites during capacitation

Protein ID	Gene name	Site	Peptide	*p* value	Fold change	Substrates of IGF1R/INSR
E9PGG4	ALS2CR11	Y53	GSEASSVPY(ph)ALNQGTTALPK	5.3E-06	Only in Cap	Yes
E9PGG4	ALS2CR11	Y1022	AEFIQEDQNMFPQDSSYY(ph)SIANK	3.1E-02	Only in Cap	
O75969	AKAP3	Y85	GFSVDY(ph)YNTTTK	2.0E-02	8.4	Yes
Q8NHS0	DNAJB8	Y53	LVSEAY(ph)EVLSDSK	3.2E-03	7.6	
Q15785	TOMM34	Y54	VLQAQGSSDPEEESVLY(ph)SNR	1.6E-02	7.5	Yes
Q9HC35	EML4	Y226	DVIINQEGEY(ph)IK	1.9E-02	5.7	Yes
P04075	ALDOA	Y364	YTPSGQAGAAASESLFVSNHAY(ph)	1.7E-03	5.3	
H0Y7A7	CALM2	Y177	EADIDGDGQVNY(ph)EEFVQMMTAK	8.5E-03	5.1	
Q5CZC0	FSIP2	Y6426	IYQVVDSVY(ph)SNILQQSGTNK	4.4E-02	5.0	
O75969	AKAP3	Y242	SFFY(ph)KEVFESR	1.3E-02	4.4	
O75952-3	CABYR	Y305	YVAMQVPIAVPADEKY(ph)QK	1.2E-02	3.7	Yes
O75969	AKAP3	Y641	LY(ph)EDDETPGALSGLTK	3.6E-02	3.6	Yes
Q5JQC9	AKAP4	Y276	IASEMAY(ph)EAVELTAAEMR	2.6E-03	3.6	Yes
Q86UC2	RSPH3	Y188	YRDSLTQPDEEPMHY(ph)GNIMYDR	9.3E-03	3.5	Yes
Q5JQC9	AKAP4	Y121	Y(ph)ALGFQHALSPSTSTCK	2.1E-02	3.4	
P26641	EEF1G	Y7	AAGTLY(ph)TYPENWR	2.9E-03	3.1	
O75969	AKAP3	Y20	VDVY(ph)SPGDNQAQDWK	2.0E-02	3.0	Yes
Q96P26	NT5C1B	Y492	FFQY(ph)DTLCESKPLAQGPLK	4.9E-02	2.9	
P00558	PGK1	Y161	LGDVY(ph)VNDAFGTAHR	2.4E-02	2.8	Yes
B7Z452	ACSL1	Y693	SQIDDLY(ph)STIKV	2.5E-04	2.6	Yes
O75969	AKAP3	Y734	GTGSAEAVLQNAY(ph)QAIHNEMR	1.0E-02	2.3	
P52565	ARHGDIA	Y156	AEEY(ph)EFLTPVEEAPK	2.6E-02	2.1	
O75969	AKAP3	Y715	LTSAFPDSLY(ph)ECLPAK	5.8E-03	2.0	Yes
P22732	SLC2A5	Y485	VSEVY(ph)PEKEELKELPPVTSEQ	2.5E-02	1.9	
H7BZL0	MKI67IP	Y12	KGIDY(ph)DFPSLVLR	3.3E-02	1.5	Yes

The fold change of "Only in Cap" means that the corresponding site is not phosphorylated in uncapacitation sperm but only becomes phosphorylated in capacitated sperm. "Site" column indicates position of phosphorylated tyrosine in protein sequences with "Y" standing for tyrosine. And "Y(ph)" means phosphorylated tyrosine in "Peptide" column.

tion sites have been quantified in mice (15) and rats (16). The quantification of phosphorylation sites in human sperm during capacitation has not been very successful (14). To better understand the regulation of phosphorylation during capacitation in humans, we performed label-free quantification of human sperm phosphorylation sites during capacitation using consecutive IMAC and TiO_2 enrichment methods. We identified 3,303 phosphorylated sites corresponding to 986 phosphorylated proteins. In capacitated sperm, the phosphorylation levels of 231 sites were up-regulated significantly, including 25 tyrosine sites.

The PhosphoSitePlus® database collects comprehensive post-translational modification information extracted from published data (30). We compared our identified sites with the PhosphoSitePlus data set and obtained an overlap of 655 sites. Thus, in sperm, there are many novel sites that are not identified in other tissues or cells (Fig. 2*D*). Previous studies have only identified a very small number of phosphorylation sites in mammalian sperm because of limitations of techniques. In human sperm, AKAP3 and AKAP4 have been shown to be tyrosine-phosphorylated during capacitation based on two-dimensional gels (14). In the present study, we also showed that the phosphorylation levels of AKAP3 and AKAP4 are significantly increased during capacitation and provided the detailed up-regulated sites (including six tyrosine sites for AKAP3 and two tyrosine sites for AKAP4). Only 30 phosphorylated peptides in mice (15) and six phosphorylated peptides in rats (16) were shown to be increased in capacitated sperm (-fold change >1.5). Because it is inappropriate to directly compare the peptides between humans and rodents, we then mapped the up-regulated peptides to gene identities. The above mouse peptides were mapped to 12 human homologous genes, and rat peptides were mapped to four human homologous genes (counting based on Entrez gene IDs). Approximately 50% of the mouse-human homologous genes (six genes) overlapped with our data set (corresponding genes with up-regulated sites), and 50% of the rat-human homologous genes (two genes) overlapped with our data set (Fig. 2*E*). For example, the phosphorylation level of the mouse homolog of AKAP4 and the rat homolog of AKAP3 was up-regulated in capacitated sperm of mice and rats, respectively. NT5C1B (5′-nucleotidase) is up-regulated in mouse and rat capacitated sperm. The enzymatic activity of 5′-nucleotidase was first verified to be up-regulated in rat sperm (16); thus, NT5C1B could be a conserved functional protein in addition to proteins of the AKAP family during sperm capacitation.

Annotation of the interacting network of proteins with increased phosphorylation levels showed complex relationships among AKAP3, AKAP4, CABYR, SPA17, and PRKAR1A. NetworKIN analysis predicted AKAP3, AKAP4, and CABYR to

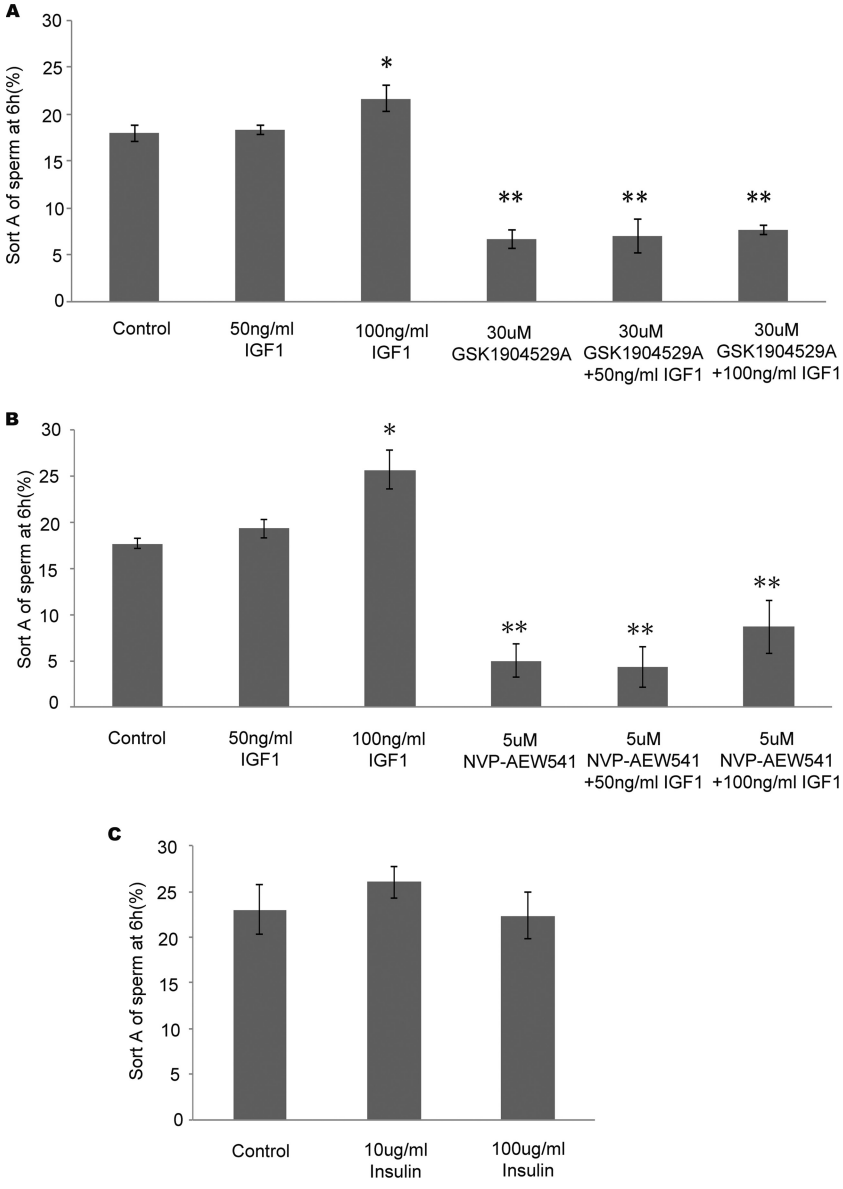

FIG. 4. **Effects of IGF1R inhibitors on hyperactivated motilities during capacitation.** *A*, hyperactivated motility was analyzed 6 h after adding different concentrations of IGF1 or GSK1904529A with DMSO as a control. *B*, hyperactivated motility was analyzed 6 h after adding different concentrations of IGF1 or NVP-AEW541 with DMSO as a control. *C*, hyperactivated motility was analyzed 6 h after adding different concentrations of insulin. *Error bars* represent S.D. *, $p < 0.05$; **, $p < 0.01$.

be substrate proteins of IGF1R/INSR kinase. AKAP3 protein is synthesized in round sperm cells, involved in the basic structure of sperm fibrous sheath, and finally located in the main segments of sperm flagellum and the acrosome region of sperm heads. AKAP3 may be involved in the regulation of sperm motility, capacitation, and acrosome reaction. AKAP3 is similar to FSP95 of which tyrosine phosphorylation occurs during human sperm capacitation *in vitro*, and the amino acid sequence has 40% similarity to AKAP4 (31). AKAP4 is a germ cell-specific protein (32) and functions in the later stages of spermatid development. AKAP4 also plays an important role in the assembly process of the fibrous sheath (33). In addition, AKAP4 is considered to be a "scaffold protein" involved in sperm flagellum movement. *Akap4* knock-out could lead to a shorter sperm flagellum and incomplete formation of the fibrous sheath, which will finally cause sperm movement disorders associated with male sterility (34). AKAP4 interacts with AKAP3 and was previously shown to have increased tyrosine phosphorylation during sperm capacitation (35). CABYR has regulatory adjuster dimerization domains, which interact with AKAP3 and AKAP4, and forms the supermolecular structure of fibrous sheath (36).

As kinases usually recognize specific sequence motifs around phosphorylation sites, it is possible to predict functional kinases based on the sequences around phosphorylation sites. According to the NetworKIN prediction database, IGF1R and INSR are the most significantly enriched kinases that interact with the up-regulated phosphorylation sites. IGF1R and INSR are from the same family and have similar structures. IGF1R and INSR share the same 13 predicted substrate phosphorylation sites. As IGF1R and INSR are both tyrosine kinases, it is possible that IGF1R or INSR may be

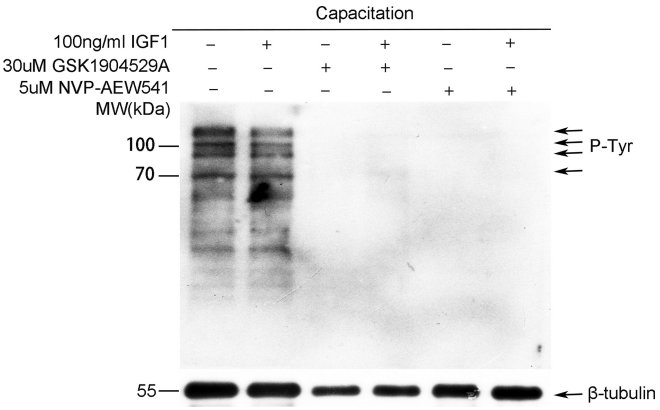

FIG. 5. **Protein tyrosine phosphorylation levels after treatment with IGF1 or IGF1R inhibitor.** Protein tyrosine phosphorylation (*P-Tyr*) levels after treatment with IGF1 (100 ng/ml), GSK1904529A (30 μM), or NVP-AEW541 (5 μM) for 6 h were evaluated by Western blotting.

essential tyrosine kinases leading to increased tyrosine phosphorylation during sperm capacitation.

The sequence similarity between IGF1R and INSR is as high as 84%. Unlike other receptor tyrosine kinases, these two receptor tyrosine kinases function on the cell surface as a homodimer comprising the same α/β-monomers or different monomers of the receptors. Once ligand binding occurs, the receptor tyrosine kinase undergoes conformational changes to bind ATP and autophosphorylate (37, 38). Autophosphorylation can enhance kinase activity of IGF1R and INSR and cause growth or metabolic reaction (39).

Hyperactivated motility is one of the hallmarks of sperm capacitation. Hyperactivated motility involves a transition in the flagellar wave from a low amplitude, symmetric beat pattern typical of progressively motile cells to a high amplitude, asymmetric thrashing of the sperm tail. A previous study suggested that this process is a cAMP-mediated event involving high levels of tyrosine phosphorylation in the sperm tail (40). Increased protein tyrosine phosphorylation is associated with hyperactivation of sperm motility. Tyrosine phosphorylation of flagellar proteins is also highly correlated with sperm hyperactivation (41).

CASA results showed that IGF1 can increase sperm hyperactivated motility, whereas insulin had no effect on hyperactivated motility, which is consistent with a previous report that IGF1 may affect sperm motility, in particular hyperactivated motility (42). IGF1 and insulin bind and activate IGF1R and INSR, respectively (43, 44). GSK1904529A is a small molecule tyrosine kinase inhibitor that can potently inhibit both IGF1R and INSR activities *in vitro* and *in vivo* by inhibiting the ligand-induced phosphorylation of IGF1R and INSR (28). NVP-AEW541 is a potent and selective IGF1R kinase inhibitor that can efficiently inhibit the growth of cells that are highly dependent on IGF1 signaling (45). Our Western blotting results confirmed that GSK1904529A and NVP-AEW541 inhibit tyrosine phosphorylation during sperm capacitation. CASA results showed that sperm hyperactivated motility was also inhibited by GSK1904529A and NVP-AEW541.

According to the literature, IGF1R plays key roles in the regulation of Sertoli cell differentiation, testis size, and follicle-stimulating hormone start-up in mice (46). Immunocytochemistry experiments indicated that IGF1R is located in the human sperm equatorial region and middle piece (47). IGF1R has been found in seminal plasma from fertile and infertile men. However, defective expression of IGF1R was observed in sperm from patients with a history of failed fertilization (48). It is possible that there might be defective hyperactive motility and tyrosine phosphorylation mediated by IGF1R during sperm capacitation in these sperm.

In conclusion, our phosphoproteomics analysis of human sperm capacitation showed that IGF1R and INSR are the most enriched tyrosine phosphorylation kinases that interacted with the up-regulated phosphorylation substrate sites during sperm capacitation. Functional assays indicated that the IGF1R-mediated tyrosine phosphorylation pathway is crucial for sperm capacitation and hyperactivated motility. As a membrane receptor tyrosine phosphorylation kinase, IGF1R could be a candidate target for contraceptives and may also be a target for improving sperm capacitation in infertile men.

* This work was supported by Chinese National Natural Science Foundation Grants 81222006, 31271245, and 31471403; 973 Program Grants 2011CB944304 and 2015CB943003; and Natural Science Foundation of the Jiangsu Higher Education Institutions of China Grant 13KJA310002.

This article contains supplemental Data 1–3.

‡ These authors contributed equally to this work.

§ To whom correspondence may be addressed. Tel.: 86-25-86862038; Fax: 86-25-86862908; E-mail: guo_xuejiang@njmu.edu.cn. and Tel.: 86-25-86862908; Fax: 86-25-86862908; E-mail: zhouzm@njmu.edu.cn.

REFERENCES

1. Austin, C. R. (1951) Observations on the penetration of the sperm in the mammalian egg. *Aust. J. Sci. Res. B* **4,** 581–596
2. Chang, M. C. (1951) Fertilizing capacity of spermatozoa deposited into the fallopian tubes. *Nature* **168,** 697–698
3. Visconti, P. E., Moore, G. D., Bailey, J. L., Leclerc, P., Connors, S. A., Pan, D., Olds-Clarke, P., and Kopf, G. S. (1995) Capacitation of mouse spermatozoa. II. Protein tyrosine phosphorylation and capacitation are regulated by a cAMP-dependent pathway. *Development* **121,** 1139–1150
4. Baldi, E., Casano, R., Falsetti, C., Krausz, C., Maggi, M., and Forti, G. (1991) Intracellular calcium accumulation and responsiveness to progesterone in capacitating human spermatozoa. *J. Androl.* **12,** 323–330
5. Naz, R. K., and Rajesh, P. B. (2004) Role of tyrosine phosphorylation in sperm capacitation/acrosome reaction. *Reprod. Biol. Endocrinol.* **2,** 75
6. Fraser, L. R. (1995) Ionic control of sperm function. *Reprod. Fertil. Dev.* **7,** 905–925
7. Garbers, D. L., Tubb, D. J., and Kopf, G. S. (1980) Regulation of sea urchin sperm cyclic AMP-dependent protein kinases by an egg associated factor. *Biol. Reprod.* **22,** 526–532
8. Tash, J. S., and Means, A. R. (1983) Cyclic adenosine 3′,5′ monophosphate, calcium and protein phosphorylation in flagellar motility. *Biol. Reprod.* **28,** 75–104
9. Carrera, A., Moos, J., Ning, X. P., Gerton, G. L., Tesarik, J., Kopf, G. S., and Moss, S. B. (1996) Regulation of protein tyrosine phosphorylation in human sperm by a calcium/calmodulin-dependent mechanism: identification of A kinase anchor proteins as major substrates for tyrosine

phosphorylation. *Dev. Biol.* **180,** 284–296
10. Mahony, M. C., and Gwathmey, T. (1999) Protein tyrosine phosphorylation during hyperactivated motility of cynomolgus monkey (*Macaca fascicularis*) spermatozoa. *Biol. Reprod.* **60,** 1239–1243
11. Lewis, B., and Aitken, R. J. (2001) Impact of epididymal maturation on the tyrosine phosphorylation patterns exhibited by rat spermatozoa. *Biol. Reprod.* **64,** 1545–1556
12. Urner, F., Leppens-Luisier, G., and Sakkas, D. (2001) Protein tyrosine phosphorylation in sperm during gamete interaction in the mouse: the influence of glucose. *Biol. Reprod.* **64,** 1350–1357
13. Nassar, A., Mahony, M., Morshedi, M., Lin, M. H., Srisombut, C., and Oehninger, S. (1999) Modulation of sperm tail protein tyrosine phosphorylation by pentoxifylline and its correlation with hyperactivated motility. *Fertil. Steril.* **71,** 919–923
14. Ficarro, S., Chertihin, O., Westbrook, V. A., White, F., Jayes, F., Kalab, P., Marto, J. A., Shabanowitz, J., Herr, J. C., Hunt, D. F., and Visconti, P. E. (2003) Phosphoproteome analysis of capacitated human sperm. Evidence of tyrosine phosphorylation of a kinase-anchoring protein 3 and valosin-containing protein/p97 during capacitation. *J. Biol. Chem.* **278,** 11579–11589
15. Platt, M. D., Salicioni, A. M., Hunt, D. F., and Visconti, P. E. (2009) Use of differential isotopic labeling and mass spectrometry to analyze capacitation-associated changes in the phosphorylation status of mouse sperm proteins. *J. Proteome Res.* **8,** 1431–1440
16. Baker, M. A., Smith, N. D., Hetherington, L., Taubman, K., Graham, M. E., Robinson, P. J., and Aitken, R. J. (2010) Label-free quantitation of phosphopeptide changes during rat sperm capacitation. *J. Proteome Res.* **9,** 718–729
17. Gandini, L., Lenzi, A., Lombardo, F., Pacifici, R., and Dondero, F. (1999) Immature germ cell separation using a modified discontinuous Percoll gradient technique in human semen. *Hum. Reprod.* **14,** 1022–1027
18. Quinn, P., Kerin, J. F., and Warnes, G. M. (1985) Improved pregnancy rate in human *in vitro* fertilization with the use of a medium based on the composition of human tubal fluid. *Fertil. Steril.* **44,** 493–498
19. Rappsilber, J., Mann, M., and Ishihama, Y. (2007) Protocol for micro-purification, enrichment, pre-fractionation and storage of peptides for proteomics using StageTips. *Nat. Protoc.* **2,** 1896–1906
20. Cox, J., and Mann, M. (2008) MaxQuant enables high peptide identification rates, individualized p.p.b.-range mass accuracies and proteome-wide protein quantification. *Nat. Biotechnol.* **26,** 1367–1372
21. UniProt Consortium (2013) Update on activities at the Universal Protein Resource (UniProt) in 2013. *Nucleic Acids Res.* **41,** D43–D47
22. Soldi, M., and Bonaldi, T. (2013) The proteomic investigation of chromatin functional domains reveals novel synergisms among distinct heterochromatin components. *Mol. Cell. Proteomics* **12,** 764–780
23. Zhou, T., Zhou, Z. M., and Guo, X. J. (2013) Bioinformatics for spermatogenesis: annotation of male reproduction based on proteomics. *Asian J. Androl.* **15,** 594–602
24. Chen, J., Bardes, E. E., Aronow, B. J., and Jegga, A. G. (2009) ToppGene Suite for gene list enrichment analysis and candidate gene prioritization. *Nucleic Acids Res.* **37,** W305–W311
25. Jensen, L. J., Kuhn, M., Stark, M., Chaffron, S., Creevey, C., Muller, J., Doerks, T., Julien, P., Roth, A., Simonovic, M., Bork, P., and von Mering, C. (2009) STRING 8—a global view on proteins and their functional interactions in 630 organisms. *Nucleic Acids Res.* **37,** D412–D416
26. Linding, R., Jensen, L. J., Pasculescu, A., Olhovsky, M., Colwill, K., Bork, P., Yaffe, M. B., and Pawson, T. (2008) NetworKIN: a resource for exploring cellular phosphorylation networks. *Nucleic Acids Res.* **36,** D695–D699
27. Morgan, D. J., Weisenhaus, M., Shum, S., Su, T., Zheng, R., Zhang, C., Shokat, K. M., Hille, B., Babcock, D. F., and McKnight, G. S. (2008) Tissue-specific PKA inhibition using a chemical genetic approach and its application to studies on sperm capacitation. *Proc. Natl. Acad. Sci. U.S.A.* **105,** 20740–20745
28. Sabbatini, P., Rowand, J. L., Groy, A., Korenchuk, S., Liu, Q., Atkins, C., Dumble, M., Yang, J., Anderson, K., Wilson, B. J., Emmitte, K. A., Rabindran, S. K., and Kumar, R. (2009) Antitumor activity of GSK1904529A, a small-molecule inhibitor of the insulin-like growth factor-I receptor tyrosine kinase. *Clin. Cancer Res.* **15,** 3058–3067
29. Chitnis, M. M., Yuen, J. S., Protheroe, A. S., Pollak, M., and Macaulay, V. M. (2008) The type 1 insulin-like growth factor receptor pathway. *Clin. Cancer Res.* **14,** 6364–6370
30. Hornbeck, P. V., Kornhauser, J. M., Tkachev, S., Zhang, B., Skrzypek, E., Murray, B., Latham, V., and Sullivan, M. (2012) PhosphoSitePlus: a comprehensive resource for investigating the structure and function of experimentally determined post-translational modifications in man and mouse. *Nucleic Acids Res.* **40,** D261–D270
31. Mandal, A., Naaby-Hansen, S., Wolkowicz, M. J., Klotz, K., Shetty, J., Retief, J. D., Coonrod, S. A., Kinter, M., Sherman, N., Cesar, F., Flickinger, C. J., and Herr, J. C. (1999) FSP95, a testis-specific 95-kilodalton fibrous sheath antigen that undergoes tyrosine phosphorylation in capacitated human spermatozoa. *Biol. Reprod.* **61,** 1184–1197
32. Fulcher, K. D., Mori, C., Welch, J. E., O'Brien, D. A., Klapper, D. G., and Eddy, E. M. (1995) Characterization of Fsc1 cDNA for a mouse sperm fibrous sheath component. *Biol. Reprod.* **52,** 41–49
33. Moretti, E., Baccetti, B., Scapigliati, G., and Collodel, G. (2006) Transmission electron microscopy, immunocytochemical and fluorescence in situ hybridisation studies in a case of 100% necrozoospermia: case report. *Andrologia* **38,** 233–238
34. Miki, K., Willis, W. D., Brown, P. R., Goulding, E. H., Fulcher, K. D., and Eddy, E. M. (2002) Targeted disruption of the Akap4 gene causes defects in sperm flagellum and motility. *Dev. Biol.* **248,** 331–342
35. Luconi, M., Cantini, G., Baldi, E., and Forti, G. (2011) Role of a-kinase anchoring proteins (AKAPs) in reproduction. *Front. Biosci.* **16,** 1315–1330
36. Johnson, L. R., Foster, J. A., Haig-Ladewig, L., VanScoy, H., Rubin, C. S., Moss, S. B., and Gerton, G. L. (1997) Assembly of AKAP82, a protein kinase A anchor protein, into the fibrous sheath of mouse sperm. *Dev. Biol.* **192,** 340–350
37. Wei, L., Hubbard, S. R., Hendrickson, W. A., and Ellis, L. (1995) Expression, characterization, and crystallization of the catalytic core of the human insulin receptor protein-tyrosine kinase domain. *J. Biol. Chem.* **270,** 8122–8130
38. Hubbard, S. R. (1997) Crystal structure of the activated insulin receptor tyrosine kinase in complex with peptide substrate and ATP analog. *EMBO J.* **16,** 5572–5581
39. Schlessinger, J. (2000) Cell signaling by receptor tyrosine kinases. *Cell* **103,** 211–225
40. Aitken, R. J., and Nixon, B. (2013) Sperm capacitation: a distant landscape glimpsed but unexplored. *Mol. Hum. Reprod.* **19,** 785–793
41. Si, Y., and Okuno, M. (1999) Role of tyrosine phosphorylation of flagellar proteins in hamster sperm hyperactivation. *Biology of reproduction* **61,** 240–246
42. Henricks, D. M., Kouba, A. J., Lackey, B. R., Boone, W. R., and Gray, S. L. (1998) Identification of insulin-like growth factor I in bovine seminal plasma and its receptor on spermatozoa: influence on sperm motility. *Biol. Reprod.* **59,** 330–337
43. Baker, J., Liu, J. P., Robertson, E. J., and Efstratiadis, A. (1993) Role of insulin-like growth factors in embryonic and postnatal growth. *Cell* **75,** 73–82
44. Liu, J. P., Baker, J., Perkins, A. S., Robertson, E. J., and Efstratiadis, A. (1993) Mice carrying null mutations of the genes encoding insulin-like growth factor I (Igf-1) and type 1 IGF receptor (Igf1r). *Cell* **75,** 59–72
45. Warshamana-Greene, G. S., Litz, J., Buchdunger, E., Hofmann, F., García-Echeverría, C., and Krystal, G. W. (2004) The insulin-like growth factor-I (IGF-I) receptor kinase inhibitor NVP-ADW742, in combination with STI571, delineates a spectrum of dependence of small cell lung cancer on IGF-I and stem cell factor signaling. *Mol. Cancer Ther.* **3,** 527–535
46. Pitetti, J. L., Calvel, P., Zimmermann, C., Conne, B., Papaioannou, M. D., Aubry, F., Cederroth, C. R., Urner, F., Fumel, B., Crausaz, M., Docquier, M., Herrera, P. L., Pralong, F., Germond, M., Guillou, F., Jégou, B., and Nef, S. (2013) An essential role for insulin and IGF1 receptors in regulating Sertoli cell proliferation, testis size, and FSH action in mice. *Mol. Endocrinol.* **27,** 814–827
47. Naz, R. K., and Padman, P. (1999) Identification of insulin-like growth factor (IGF)-1 receptor in human sperm cell. *Arch. Androl.* **43,** 153–159
48. Sánchez-Luengo, S., Fernández, P. J., and Romeu, A. (2005) Insulin growth factors may be implicated in human sperm capacitation. *Fertil. Steril.* **83,** 1064–1066